Energy xxx (2014) 1–13

Contents lists available at ScienceDirect

Energy

journal homepage: www.elsevier.com/locate/energy

Improving the energy storage capability of hot water tanks through wall material specification

P. Armstrong*, D. Ager, I. Thompson, M. McCulloch

Department of Engineering Science, Begbroke Science Park, Oxfordshire OX5 1PF, UK

ARTICLE INFO

Article history:
Received 3 March 2014
Received in revised form
15 September 2014
Accepted 18 September 2014
Available online xxx

Keywords:
Thermal stratification
Domestic hot water tank
Demand side management
Computational fluid dynamics
Material selection

ABSTRACT

Domestic hot water tanks represent a significant potential demand side management asset within energy systems. To operate effectively as energy storage devices, it is crucial that a stratified temperature distribution is maintained during operation; this paper details experimental and numerical work conducted to understand the influence that wall material specification has on de-stratification within domestic hot water tanks. A 2d axisymmetric CFD (Computational Fluid Dynamic) model was consistent with experiments which showed that switching from copper to stainless steel resulted in a 2.7 fold reduction in useable hot water loss through reduced de-stratification for a 74 L UK domestic hot water tank over a 48 h period. During simulation, a counter rotating convection system, with peak velocities of 0.005 m/s, was observed above and below the thermocline. Minimizing de-stratification, through appropriate wall material selection, increases the performance of hot water tanks and scope for their use in demand side management applications. Given the inconclusive evidence surrounding copper's efficacy as a sanitizing agent, along with the low tensile strength of polyethylene, this paper advocates the use of stainless steel in hot water tank walls and further exploration of alternative materials and composites which have low cost and low thermal conductivity along with high strength and manufacturability.

1. Introduction

Domestic hot water usage is responsible for between 17 and 39% of household energy demand [1,2]; consequently, domestic hot water tanks represent a potentially significant source of energy storage to accommodate the large and intermittent demands of instantaneous power that occur throughout the day in a typical dwelling [3]. The transition towards renewable energy sources has led to an increased focus on the potential application of demand side management strategies for electric domestic hot water systems [4,5]. Off peak connection of domestic hot water heating elements has been a routine measure in the UK since 1978 to efficiently utilize conventional base-load power plant such as coal and nuclear [6]. Atikol et al. found that in North Cypress, demand side management of electric hot water tanks could potentially delay the procurement of peaking generation equipment, saving over ten million dollars in capital costs alone [5]. In Lebanon, a recent lifecycle analysis recommended the use of renewable energy sources to directly provide domestic hot water which is the largest consumer of primary energy within homes in the country [7]. In addition to this, an economic analysis of load management within the German residential sector has shown that thermal energy storage for domestic hot water and space heating is key to realizing the targets associated with the country's transition to renewable energy sources, or Energiewende [8].

Simple, fixed-volume hot water tanks, exploiting natural thermal stratification, provide an economic means of storing energy [9,10], and are an attractive proposition given the challenges associated with other forms of energy storage, such as: flywheels, super-capacitors and batteries [11]. Flywheel's have to be constructed from composite materials to absorb energy in the event of the assembly disintegrating and require a partial vacuum and high efficiency bearings to avoid excessive rates of self-discharge; a recent prototype trialed for home energy storage in sub-Saharan Africa had to work in tandem with lead acid batteries to be viable [12]. Battery based energy storage systems are problematic in that they rely on materials that are either toxic in the case of lead acid batteries or volatile in the case of Lithium Ion cells [13]; whilst Lithium Ion chemistries achieve far higher energy densities than lead acid systems, they rely on a more elaborate battery management system to avoid thermal runaway which can lead to electrical fires [14]. Supercapacitors, often touted as the future substrate for energy storage on account of high cycle life, reliability and a low

* Corresponding author.
E-mail address: Peter.armstrong@eng.ox.ac.uk (P. Armstrong).

http://dx.doi.org/10.1016/j.energy.2014.09.061

Nomenclature

Parameter, symbol, units

ambient temperature T_a, °C
analytical wall temperature T_2, °C
analytical water temperature T_1, °C
average tank vertical velocity v, m/s
axial wall flux Q_{aw}, W
cost function input features a,b,c, NA
cross sectional area A, m^2
density ρ, kg/m^3
dimensionless time t^*, NA
Fourier number F_o, NA
Grashoff number G_r, NA
gravitational acceleration g, m/s^2
gravitational acceleration g, m/s^2
heat capacity C_p, J/kgK
initial tank temperature T_s, °C
inlet water temperature T_c, °C
internal energy E_j, J
internal exergy Ex, J
internal tank pressure P, Pa
kinematic viscosity υ, m^2/s
local wall water temperature difference ΔT, K
mass m, kg
Nusselt number N_u, NA
Prandtl number P_r, NA
radial wall heat flux Q_r, W
Rayleigh number R_a, NA
tank circumference l, m
tank diameter d, m
tank height H, m
tank radius r, m
tank wall hoop stress σ_h, Pa
tank wall longitudinal stress σ_l, Pa
tank wall thickness T, °C
tank wall Von Mises stress σ_{VM}, Pa
thermal conductivity k, W/mK
time t, seconds
useable volume V_u, liters
useful temperature threshold T_u, °C
vertical coordinate in tank x, m
volumetric expansion coefficient β, 1/K
water temperature $T(x)$, °C

environmental foot-print [15,16], at present suffer from achieving relatively low energy densities, high rates of self-discharge and efficiency penalties associated with the power electronics required to manage the change in terminal voltage against state of charge during operation [17]. Tanks of heated water or water-glycol can store energy with a near indefinite cycle life, low environmental footprint and low cost. A 120 L tank purchased in the UK represents a cost of approximately 50 $/kWh[1] compared with 120 $/kWh and 600 $/kWh for lead acid and lithium ion respectively [18]. If we consider the dry weight of a hot water tank, a higher specific energy density is achieved in terms of the mass of materials used in its construction at 0.47 kWh/kg compared with 0.04 kWh/kg and 0.15 kWh/kg for lead acid and lithium ion.

Effective operation of hot water stores relies on natural thermal stratification [20]. Stratification, which arises as water density changes with temperature [21], ensures that a stable outlet and/or heat exchanger temperature is maintained; this reduces the requirement for cyclic firing of heating elements and lowers standing heat losses [10,22]. De-stratification will compromise the system's ability to utilize flexible tariff schemes and ultimately reduces the extent to which variable sources of renewable energy can be accommodated. In the case of solar fired hot water systems, thermal stratification ensures that the return temperature to the collector is minimized during operation improving the overall heat transfer from the collector-tubes to the water and increasing the number of hours over the day during which the system can operate effectively [23].

Much work has been undertaken to understand the design features that promote thermal stratification and minimize de-stratification during operation. In Ref. [22], the role of the Richardson's number, which expresses the ratio of potential to kinetic energy within stratified water, was identified. During 'dynamic mode operation', where hot water is drawn from the tank, stratification breaks down as flow rates increase and the Richardson's number drops [24], this can be observed in experiments where the vertical temperature distribution is monitored over time [25]. Increasing the tank's aspect ratio (height/diameter) reduces dynamic mode de-stratification at the expense of elevated heat losses [26] with an optimum value being somewhere between 3 and 4, a range confirmed experimentally in Ref. [27].

This paper's focus is on how the materials selected for the inner wall of a tank contribute to de-stratification during a tank's 'static-mode' of operation. Whilst the tank stands unused, holding heat on standby, de-stratification arises due to both heat losses and vertical conduction, this can be observed experimentally in Ref. [28].

To predict rates of static-mode de-stratification, Abdoly et al. applied a radial conduction model to the water and wall volumes within a hot water tank. The model under-predicted the rates of de-stratification that occurred during experiment, the authors hypothesized that this was due to eddy currents occurring around the thermocline region which were neglected and that a thinner wall would have led to reduced rates of de-stratification [29]. Commercial one dimensional stratification models include an additional heat transfer term to account for this source of de-stratification [30]. Further detail of the phenomenon was revealed by CFD (Computational Fluid Dynamic) analysis which indicated buoyancy driven flows arising close to the tank wall [31]. Fan et al. have shed light on the global flow pattern throughout a de-stratified tank with their analysis [23], however there has been little emphasis on the local flow phenomenon occurring around the thermocline for a stratified temperature distribution and how this influences local heat transfer correlations. The extent to which de-stratification is influenced by wall material selection has also not been explored.

The thermal conductivity of any wall material that is selected for a hot water tank will have a bearing on the rate of static mode de-stratification. Historically, hot water tanks in the UK have been made of copper [32] which has a thermal conductivity that is approximately 40 times greater than stainless steel. The reason that copper is so widely used is that it is a malleable material which is easy to machine and has low rates of corrosion along with perceived antimicrobial qualities [33]. However, in spite of this perception, it was found in Ref. [34] that of 457 hot water systems

[1] Assuming a 117 L BS7[e] UK hot water tank operating at 60 °C with an inlet temperature of 20 °C. Example unit sourced from RMCylinder.com.

Please cite this article in press as: Armstrong P, et al., Improving the energy storage capability of hot water tanks through wall material specification, Energy (2014), http://dx.doi.org/10.1016/j.energy.2014.09.061

sampled for *Legionella,* a pathogen associated with Legionnaire's disease [35], systems plumbed in copper were in fact more frequently associated with contamination. In two separate studies of student apartments, prolific bacterial growth was found in the bottom of domestic copper tanks [20,36]. Given that the sanitary performance of copper-walled hot water tanks is debatable, this paper explores the implications that alternative material choices would have on thermal performance.

We begin by considering the criteria associated with tank wall material selection in Section 2 allowing us to narrow the choice of candidate options for analysis in subsequent sections. To quantify the relative thermal performance of these choices, Section 3 introduces the metrics used to assess rates of internal destratification. Section 4 discusses the limitations associated with one-dimensional analytical and numerical approaches which leads into Section 5 which details an experimentally validated 2d CFD model. This model is validated through laboratory testing described in Section 6. Both experimental and numerical results are presented in Section 7 to inform a discussion and conclusions in Section 8.

2. Wall material selection criteria

When specifying the tank wall material, a number of criteria including: cost, compatibility with potable water, mechanical properties and thermal performance will have to be considered. We deal with each of these in turn:

2.1. Material cost

Table 1 shows the prices associated with the materials considered in this paper. In recent years the price of copper has fluctuated between $3000 and $10,000 USD/ton and is presently worth $7000 USD/ton [37]. Between September 2012 and January 2013, stainless steel has averaged $2800 USD/ton and peaked at $3000 USD/ton, or roughly half the price of copper [38]. Polyethylene, a plastic used in potable hot water applications [33], traded for between $1500 and $1700 USD/ton throughout 2013 [39] making it about half the price of stainless steel.

2.2. Compatibility with potable water

Any wall material in contact with potable water will have to withstand corrosion and should not promote the growth of biofilms which can host human pathogens. Heavy bacterial colonization has been associated with certain rubbers, silicones and aluminum [40–42] whilst Aluminum has been associated with the onset of neurological disorders such as Alzheimer's [43,44]. There is conflicting evidence around copper's potency against bacteria; one laboratory study found copper to exhibit lower growth rates than other plumbing materials [45] however this is contradicted by Ref. [34] where a positive correlation between copper walled tanks and *Legionella* growth was observed.

2.3. Mechanical properties

Copper is malleable and straightforward to work whereas stainless steel is harder to drill and welds at higher temperatures requiring more sophisticated manufacturing processes [46]. Whilst Polyethylene can be joined easily at low temperatures, its relatively low tensile strength limits its application without reinforcement from other materials within a composite assembly. Composite pressure vessels have been developed where a pre-tensioned continuous filament winding is wrapped around an inner liner material to achieve high strength and low weight [47]. Given the relatively low pressures that domestic hot water systems operate at, composite wall structures will not be considered in this paper.

The maximum operating pressures for unvented UK hot water systems is 6.5 bar [48]. The wall thickness will be specified in order to withstand the associated stresses at this pressure. When the ratio of wall thickness, T, to vessel radius r, within a cylindrical vessel falls beneath 1/20, membrane stress theory can be applied to resolve the Von Mises stresses, σ_{VM}, that occur by calculating the longitudinal and hoop stresses, σ_l and σ_h, that prevail [49]:

$$\sigma_h = \frac{P.r}{T} \tag{1}$$

$$\sigma_l = \frac{P.r}{2T} \tag{2}$$

$$\sigma_{VM} = \sqrt{\sigma_h^2 - \sigma_h\sigma_l + \sigma_l^2} \tag{3}$$

where: P is the pressure within the tank.

Whilst the above analysis provides a good approximation of the stresses for the vertical wall sections, stress concentrations arise where the geometry changes towards the top and bottom ends of the tank; this is reflected in the British design standard for vented cylinders which specifies a thicker grade of copper for the top and bottom dome sections [32]. To optimize the thickness of wall material across the entire cylinder, finite element stress analysis is required [50].

The stresses that prevail within the tank wall will be determined by both the operating pressure and tank diameter. In the UK, the average hot water consumption is 122 L/day [19]; this can be satisfied by a UK BS8^e tank which has a diameter of 450 mm [32]. The amount of wall material required can be calculated using equations (1)–(3) and through reference to gauge requirements specified in BS7206:1990 [48]. Table 2 shows these gauge requirements translated into costs against operating pressure for a BS8^e tank operating over the range of standard operating pressures in the UK.

Table 1 shows the tensile strength associated with the main wall material options. Cross linked polyethylene has the lowest tensile strength of between 14 and 40 MPa [51] rendering it unsuitable on its own. However, there may be scope for its use if reinforced by other materials; for instance a glass reinforced fiber plastic tank,

Table 1
Materials and their associated parameters considered in this paper.

Material	Strength (MPa)	Thermal conductivity (W/mK)	Manufacturability	Material cost ($/ton)	Properties reference
Copper C106	200–300	398	Malleable, welds at low temperatures	7000	[55,56]
Stainless steel (UNS444000)	415	26.8	More difficult to machine, requires more sophisticated welding processes	3000	[48,57]
Cross linked polyethylene	14–40	0.33	Joins at low temperatures though requires additional materials to withstand operating pressures	1600	[51,58]
Rigid polyurethane insulating foam	NA	0.028	NA	NA	[59]

Please cite this article in press as: Armstrong P, et al., Improving the energy storage capability of hot water tanks through wall material specification, Energy (2014), http://dx.doi.org/10.1016/j.energy.2014.09.061

Table 2
Cost of wall materials against operating pressure for a 144 L cylindrical tank.

Operating pressure (bar)	Stainless cost ($)	Copper cost ($)	Polyethylene liner cost ($)
2.5	26.5	90.2	3.4
3.5	26.5	140.3	3.4
4.5	28.4	180.4	3.4
5.5	34.1	220.5	3.4
6.5	39.8	260.6	3.4

designed to capture heat effectively from a solar collector has been tested recently in Nigeria [52].

In addition to the material options discussed so far, some manufacturers produce tanks using a vitreous enamel coating applied to steel, however the enamel is prone to cracking due to thermally induced stresses meaning that sacrificial anodes are required and a shorter lifespan can be expected compared to stainless steel [53].

2.4. Thermal performance

Domestic hot water tank walls range in thickness by between 0.5 and 2.6 mm [32,48]. Being thin and metallic, the inner wall has little influence on heat losses which are determined primarily by the external insulation cladding. Typically, a 50 mm thick layer of rigid polyurethane foam is applied to domestic tanks in the UK. However, it has been observed that a significant fraction of the heat flux conducted vertically during de-stratification is through the metal tank inner walls and convection currents adjacent to them [26,31,54], it is this mechanism that will be explored in later sections of this paper.

2.5. Summary table

Table 1 summarizes the three wall materials that will be analyzed. The insulation foam applied to the experimental test tanks, detailed in Section 6, is also included.

3. Evaluating rates of de-stratification

One of the primary objectives of a hot water tank is to maintain the availability of heat during operation. Consequently, the extent to which heat is degraded over time needs to be quantified. This section discusses a range of metrics that can be used to evaluate the influence of different wall materials and grades on rates of standing de-stratification.

Fig. 1 illustrates the temperature distribution through a hot water cylinder:

In Ref. [10], water based thermal energy storage systems are assessed on the basis of Exergetic performance. Exergy is defined as the maximum amount of useful work that can be extracted from a unit of energy within its environment [60]. We can track the loss of Exergy occuring within the tank over time for a vertical temperature distribution throughout a tank, $T(x)$, with respect to the ambient temperature T_a assuming constant cross sectional area, pressure and heat capacity using equation (4). Whilst we assume that $T(x)$ describes each horizontal temperature band for a given vertical position, there will be areas close to the walls and thermocline region where unsteady spatial variations in horizontal temperature distribution arise due to convection, it is assumed that these regions account for a negligible fraction of the overall volume of water within the tank, an assumption which is consistent with the widespread application of isothermal nodes used in one-dimensional stratification models [61–63]. Since measurable rates

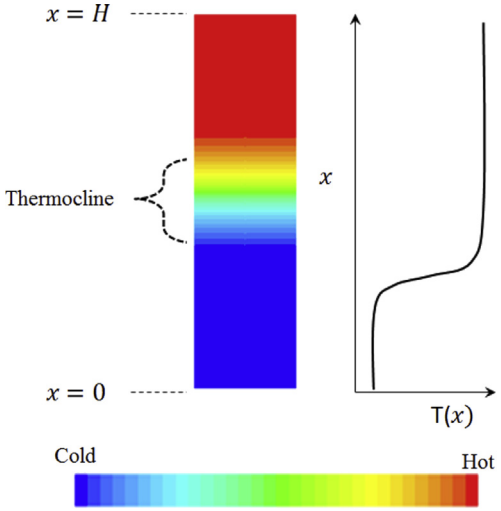

Fig. 1. Cross section illustrating temperature distribution through a hot water cylinder annotated to show thermocline region.

of de-stratification occur over relatively long timescales of hours or more [64], we assume that for any instant in time, the system can be measured with the assumption that the conditions are at steady state, in other words there is no significant error associated with the transient nature of $T(x)$ which only appears over long timescales.

$$Ex(t) = mC_p \int_0^H (T(x) - T_c)\left[1 - T_a/T(x)\right]dx \tag{4}$$

An alternative metric, referred to as useable volume, V_u [20], quantifies the volume of fluid from a tank that can be mixed to a useful final operating temperature, T_u. For domestic applications, T_u is typically between 41 °C to 44 °C, depending on whether the application is bathing or showering [65] and will be assumed to be 43 °C throughout this paper. The amount of useable volume within a tank can be computed as follows:

$$V_u(t) = m \int_{x \text{ at } T(x)\geq T_u}^{H} 1 + \frac{T(x) - T_u}{T_u - T_c}dx \tag{5}$$

where T_c is the inlet water temperature.

To distinguish between heat loss and de-stratification, the energy content within the tank, E_j, can also be deduced for an ambient temperature, T_a.

$$E_j = mC_p \int_0^H (T(x) - T_a)dx \tag{6}$$

If we consider a tank in static mode after heating, the rate of Exergy destruction, useable volume destruction and energy loss, can be evaluated by computing equations (4)–(6) at two intervals, occurring at t_1 and t_2:

$$\dot{E}_{x,\text{ destroyed}} = \frac{E_x(t_2) - E_x(t_1)}{t_2 - t_1} \tag{7}$$

$$\dot{V}_{u,\text{ destroyed}} = \frac{V_u(t_2) - V_u(t_1)}{t_2 - t_1} \tag{8}$$

$$\dot{E}_{j,\text{ lost}} = \frac{E_j(t_2) - E_j(t_1)}{t_2 - t_1} \tag{9}$$

The output of equations (7) and (8) will be used in later sections of this paper to assess the relative performance of copper and

Please cite this article in press as: Armstrong P, et al., Improving the energy storage capability of hot water tanks through wall material specification, Energy (2014), http://dx.doi.org/10.1016/j.energy.2014.09.061

stainless steel over time for both the experimental and numerical analysis that has been undertaken.

4. One dimensional analytical and numerical treatment

To compute equations (4)–(6), a model is required to determine the vertical temperature distribution, $T(x)$ and its evolution over time. A coupled heat equation forms the basis of a one dimensional model formulated in Ref. [22] for the purpose of developing analytical formula that describe thermal stratification within a vertical cylinder. The analysis begins by considering heat transfer between the tank water and wall volumes using equations (10) and (11):

$$k_1 A_1 \frac{\partial^2 T_1}{\partial x^2} - \rho_1 C_{p1} A_1 v - \rho_1 C_{p1} A_1 \frac{\partial T_1}{\partial t} = -h(x) l (T_2 - T_1) \tag{10}$$

$$k_2 A_2 \frac{\partial^2 T_2}{\partial x^2} - \rho_2 C_{p2} A_2 \frac{\partial T_2}{\partial t} = h(x) l (T_2 - T_1) \tag{11}$$

where: subscripts 1 and 2 refer to water and wall properties respectively, C_p is the specific heat capacity, ρ is density, k is thermal conductivity, T_1 and T_2 stand for temperatures as a function of position x for both the water and wall volumes, A is the cross sectional area, v is the average vertical flow velocity through the tank which is zero for static mode operation, x is the vertical position as shown in Fig. 1 and l is the tank circumference.

Of particular interest is the parameter $h(x)$ which denotes the local film heat transfer coefficient between the wall and water. Since $h(x)$ couples equations (10) and (11), analytical solutions were not available to the authors in Ref. [22]. However an analytical solution with empirical coefficients was derived on the assumption that vertical conduction through the wall was negligible ($k_2 = 0$). However, both numerical and experimental work discussed in this paper demonstrates that vertical conduction through the wall has a highly significant influence on the rate of de-stratification within the tank.

Given the limitations associated with analytical approaches, a numerical approach to equations (10) and (11) could be taken if an appropriate function describing $h(x)$ can be found. An averaged Nusselt number for a heated vertical cylinder is presented in Ref. [66], however the authors of this paper could find no correlations that relate to a conductive vertical geometry which is immersed in a stratified fluid. One correlation, presented in Ref. [67], relates specifically to a cylinder which is cooled at the top and heated from the bottom where the wall is assumed to be either a perfect insulator or conductor of heat meaning that it could not be applied for this application where the conductivity of the wall changes depending on the material selection. A one dimensional stratification model called TRNSYS, which is used extensively in the literature [62,68–71], makes use of an extra conduction term in the energy balance for each node to account for the influence of convection currents around the wall [54]. However, this conduction term has to be derived empirically.

5. CFD model

Given the limitations associated with one dimensional approaches, along with the lack of relevant heat transfer correlations in the literature, a CFD model was developed to provide further insight. 3D CFD simulations were found to agree with experimental results presented in Refs. [31] and [72]. To reduce simulation time, the model in this paper comprises of a 2D axi-symmetric section which is simulated using the finite volume method [73] in the StarCCM+™ software environment [74]. To implement an axisymmetric model, the governing equations associated with each node in the mesh are expressed in cylindrical coordinates [75]; an example of this approach is given in Ref. [76].

A polyhedral mesh was used to simulate the wall and water volumes associated with the stainless test tank detailed in Section 5, Fig. 2. A 2nd order solver using a simulation time step of 1 s was used. The Boussinesq approximation, where: the density is assumed to be constant along with all other fluid properties, viscous dissipation is assumed to be negligible and an additional buoyancy force term is included in the momentum equation which takes account of the thermal expansion of water with temperature was applied [77]. The domain over which the Boussinesq approximation is valid has been provided by Gray and Giorcini [78].

Table 3 provides a summary of the model and hardware used during simulation whilst Fig. 2 shows the polyhedral mesh applied to an axisymmetric section of the Stainless tank Geometry.

The initial temperature distribution throughout the CFD model was derived from the experimental measurements detailed in Section 5. An appropriate interpolant function had to be chosen so that all values throughout the mesh could be initialized. The following analytical solution to equations (10) and (11) for a stratified temperature distribution, derived in Refs. [22], was used [79]:

$$\frac{T(x) - T_c}{T_s - T_c} = \frac{1}{2}\left[1 + \mathrm{erf}\left(\frac{\frac{x}{L} - \frac{t}{t^*}}{2\sqrt{F_o}\sqrt{\frac{t}{t^*}}}\right)\right] \tag{12}$$

where, T_s is the initial temperature throughout the tank, L is the height of the tank, F_o is the Fourier number and t^* is the system time constant.

To fit equation (12) to the measured temperature distribution, the hypothesis function described by equation (13) was developed from Ref. [9] where coefficients a, b and c were input features to the non-linear least squares cost function which was minimized with respect to $T(x)$ for measurements $T(n)$. This procedure was undertaken in the Matlab™ environment and a detailed description can be found in Refs. [80,81]:

$$T(x) = \alpha\left[1 + \mathrm{erf}\left(\frac{\frac{x}{L} - a}{b}\right)\right] + T_c + c \tag{13}$$

where:

$$\alpha = \frac{T_s - T_{in}}{2} \tag{14}$$

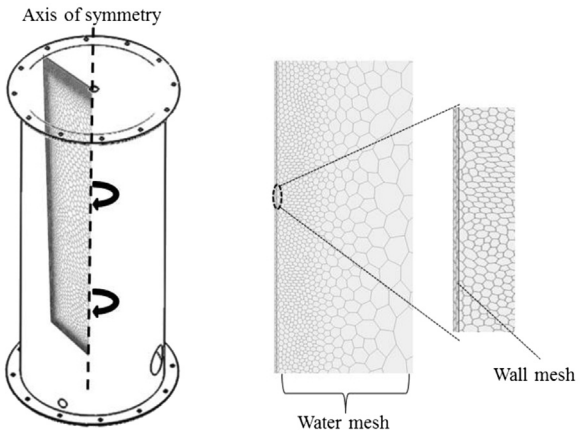

Fig. 2. (Left) drawing of stainless test tank (middle) axi-symmetric polyhedral mesh (right) detailed view of wall mesh.

Please cite this article in press as: Armstrong P, et al., Improving the energy storage capability of hot water tanks through wall material specification, Energy (2014), http://dx.doi.org/10.1016/j.energy.2014.09.061

Table 3
Details of CFD Model used in this paper.

CFD model parameter	Value
Model	Laminar
Solver	2nd order
Simulation time step	1 s
Mesh type	Polyhedral
Run time	10.8 s simulation time for 1 s real time (4 h 27 min for 48 h simulation)
Platform details	Processor: Intel i3-2100 3.1 GHz 8 GB of RAM

6. Experimental work

6.1. Description of apparatus

An experiment with two objectives was conducted. Firstly, the CFD model described in Section 5 needed to be initialized and validated so that a wider exploration of alternative material options could be explored. Secondly, a direct comparison of the static mode de-stratification rate for a commercially available domestic tank made in copper and an equivalently sized stainless steel unit was to be made. This was to test the hypothesis that de-stratification would be less pronounced for stainless cylinder walls due to the lower thermal conductivity compared to copper walls (see Table 1).

Two tanks with a volume of 74 L and diameter of 350 mm were tested (Fig. 3). One tank was made from 1 mm thick stainless steel (type UNS444000 specified in Ref. [48]) whilst the other was a commercially available British Standard BS7 tank made from 0.7 mm thick copper (type C106) as specified in Ref. [32]. The stainless tank was 790 mm high whilst the copper tank was 900 mm tall but with the same volume because of domed top and bottom features which conform to British Standard 699:1984 [32]. Both cylinders had a 57 mm immersion port centered half way up the side of the tank wall to accommodate a 3 kW direct 279 mm immersion heating element. Prior to being sprayed with 50 mm of polyurethane rigid insulating foam, both tanks were fitted with an array of 8 internal temperature probes comprising M5 nylon bolts which were center drilled to accommodate T-type thermocouple temperature sensors. Each probe assembly was inserted such that the thermocouple junction was immersed in the water at a distance of 50 mm ± 5 mm radially from the tank wall. The probe intervals were spaced at isochoric intervals as shown on Fig. 4 and consistent with the experimental procedure undertaken in Ref. [20].

The experimental procedure involved turning both immersion elements on at the same time until the thermostats reached 60 °C at which point they were shut off. The vertical temperature distribution was then measured for a period of 48 h as the tanks de-stratified and lost heat to their surroundings. The temperature distribution, recorded immediately after the point at which the heating elements were shut off, was used to initialize the CFD simulation detailed in Section 5.

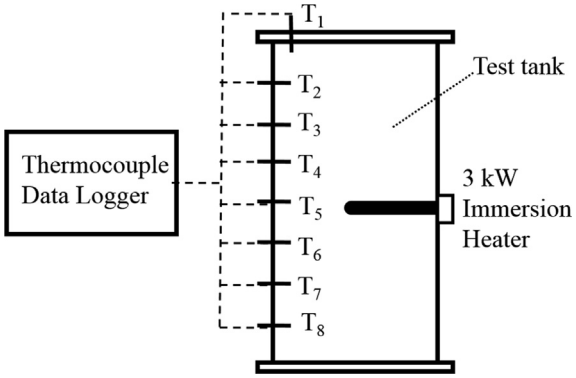

Fig. 4. Section view of BS7 copper cylinder showing temperature sensor placement.

6.2. Error analysis

Errors can be considered in quadrature where measurements are made independently of each other allowing for more precision to be assumed [82]. However, the thermocouples used in this experiment made use of a single cold reference for each tank meaning a potential common source of error and therefore a more conservative approach to the analysis has been taken. The maximum error associated with each parameter has been assumed and applied such that the worst possible band of uncertainty $+Err(param) \leftrightarrow -Err(param)$ can be determined for equations (4)–(6). Equations (15) to (20) show how this is implemented for errors in temperature, ΔT, and water mass measurements Δm for exergy, energy and useable volume measurements.

$$+\mathrm{Err}(E_x(x)) = [m + \Delta m] C_p \int_0^H ([T(x) + \Delta T] - [T_c - \Delta T]) \left[1 - \frac{[T_a - \Delta T]}{[T(x) + \Delta T]}\right] dx \quad (15)$$

Fig. 3. (Left) Stainless steel tank, (center) copper tank, (right) insulated tanks under test.

Please cite this article in press as: Armstrong P, et al., Improving the energy storage capability of hot water tanks through wall material specification, Energy (2014), http://dx.doi.org/10.1016/j.energy.2014.09.061

$$-\mathrm{Err}(E_x(x)) = [m-\Delta m]C_p\int_0^H([T(x)-\Delta T]-[T_c+\Delta T])\left[1-\frac{[T_a+\Delta T]}{[T(x)-\Delta T]}\right]dx \quad (16)$$

$$+\mathrm{Err}(E_j(x)) = [m+\Delta m]C_p\int_0^H([T(x)+\Delta T]-[T_c-\Delta T])dx \quad (17)$$

$$-\mathrm{Err}(E_j(x)) = [m-\Delta m]C_p\int_0^H([T(x)-\Delta T]-[T_c+\Delta T])dx \quad (18)$$

$$+\mathrm{Err}(V_u(x)) = [m+\Delta m]\int_{x\ \text{at}\ T(x)\geq T_u}^H 1+\frac{[T(x)+\Delta T]-T_u}{T_u-[T_c+\Delta T]}dx \quad (19)$$

$$-\mathrm{Err}(V_u(x)) = [m-\Delta m]\int_{x\ \text{at}\ T(x)\geq T_u}^H 1+\frac{[T(x)-\Delta T]-T_u}{T_u-[T_c-\Delta T]}dx \quad (20)$$

The errors were added to the measurements before the interpolant function was applied to the integral within the above equations.

The thermocouple readings were all found to be within ± 0.5 °C of a 5 point UKAS calibrated platinum resistance thermometer reference with quoted accuracy of ± 0.05 °C within a stirred water calibration bath. A set of digital scales recorded the water mass to within ± 0.1 kg. This yields worst case errors of ± 0.01 kWh and ± 0.09 kWh on application of equations (15)–(18).

Estimating the uncertainty associated with V_u is less straightforward due to the lower limit on the integral term in equations (5), (19) and (20). The upper and lower bounds for V_u are therefore calculated across the entire duration of the experiment and shown alongside the results on Fig. 5d.

7. Results

This section presents the results of the experimental and numerical analysis, we begin by presenting the experimental data from the test detailed in Section 6, this was used to initialize the CFD model described in Section 5. Once validated by experiment, the CFD model was used to explore the flow pattern within the tank along with a number of alternative wall material options the results of which are detailed towards the end of this section.

7.1. Experimental results

The measured temperature distribution over time for the copper and stainless tanks is shown by Fig. 5 (a) and (b). After warm up, the temperature distributions within both tanks were nearly identical with initial exergy and useable volume values being within 0.2% and 0.6% of each other with initial values of 1.077 MJ compared to

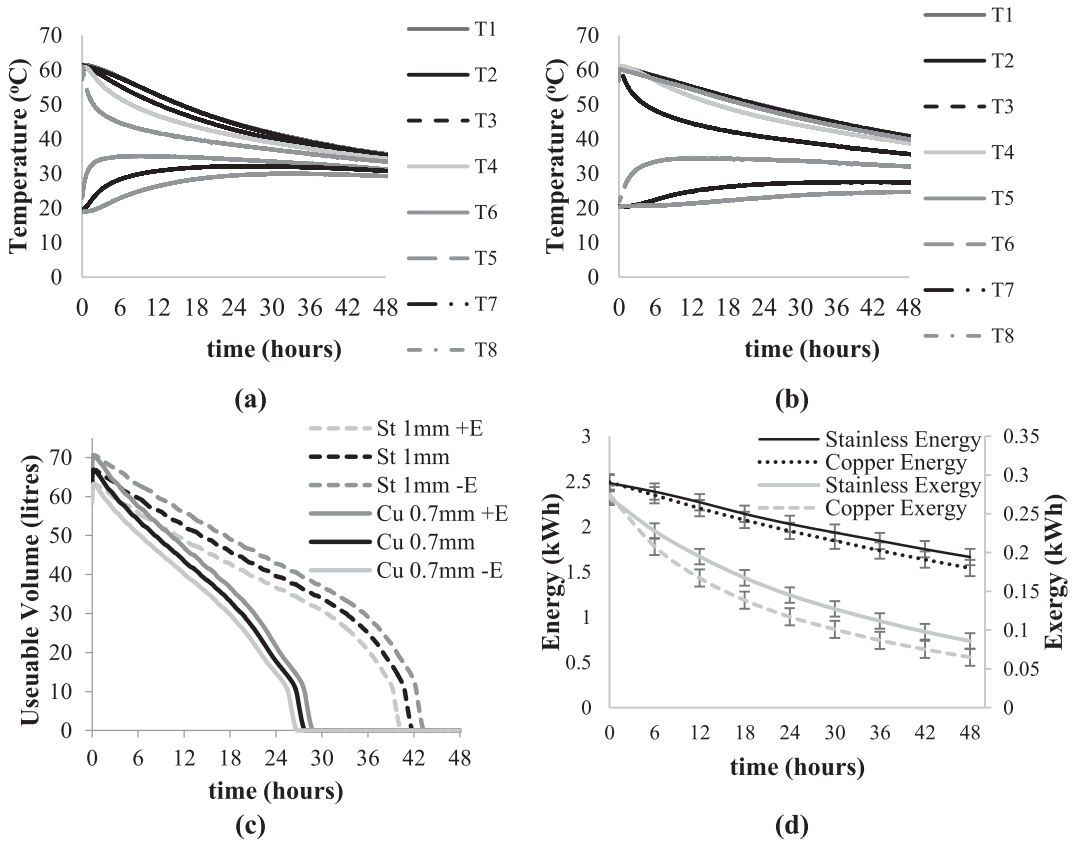

Fig. 5. Experimental results: (a) vertical temperature distribution over time for the copper tank, (b) vertical temperature distribution over time for the stainless tank, (c), change in useable volume over time for both copper and stainless tanks where +E and −E denote values associated with maximum error (d) changing internal exergy and energy for both the copper and stainless tanks.

Please cite this article in press as: Armstrong P, et al., Improving the energy storage capability of hot water tanks through wall material specification, Energy (2014), http://dx.doi.org/10.1016/j.energy.2014.09.061

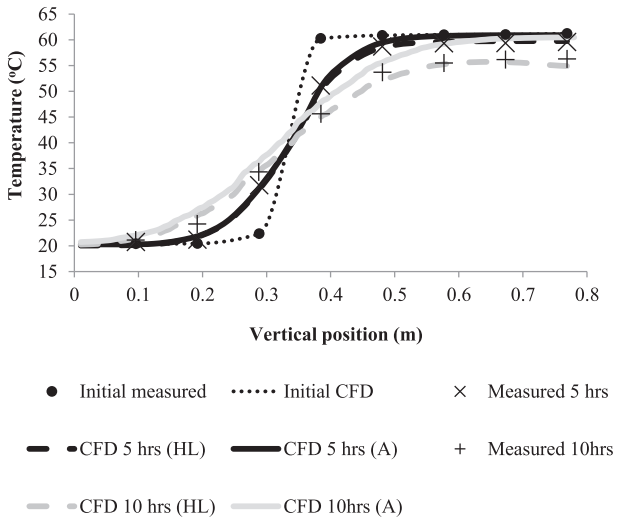

Fig. 6. Evolution of vertical temperature distribution from initial condition after, 5, 10 and 20 h against CFD model. (HL) = model where heat losses to ambient are included, (A) shows CFD model output for adiabatic system.

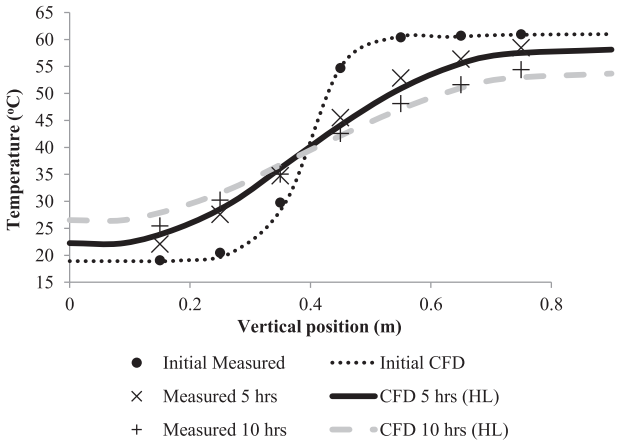

Fig. 7. Evolving temperature field against CFD simulation for copper tank.

1.075 MJ and 65.4 compared to 65 L for the stainless and copper units respectively. Comparing Fig. 5 (a) and (b) over the 48 h period, de-stratification is much more rapid in the copper cylinder as can be seen by the more rapid convergence of temperatures. The results of this are evident in Fig. 5 (c) which shows the change in useable volume over time; all useable hot water, for a threshold temperature of 43 °C, was lost in the copper cylinder by 28 h (±1 h) compared to 42 h ($\pm 1^1/_2$ h) for the stainless tank. After 24 h, the copper tank had 24% less exergy than the stainless tank, as the temperatures converge, the disparity between the two tanks reduce such that by 48 h measurement error bounds overlap one another (Fig. 5 (d)).

For the first 12 h, the relationship between useable volume loss and time for both the copper and stainless tanks were linear with values of 2.1 L per hour ($R^2 = 0.95$) and 1.18 L per hour ($R^2 = 0.98$) respectively (Fig. 5(c)). This linearity breaks down in the hours towards total loss of useable volume.

7.2. CFD results

Here we show the CFD results. Before exploring the resulting vector fields and de-stratification rates for different wall material choices, we first verify the output of the model against the stainless and copper test tanks by examining Fig. 6. Simulated temperatures from reference mesh node center positions, which were within 1.5% of the vertical position of temperature sensors 1 to 8 and 5 mm from the tank wall, were extracted and compared with experimental results. The temperature distribution for both the initial state after warm-up along with the states after 5 h and 10 h for the stainless tank and CFD output are shown. The model and experiment agreed within the ± 0.5 °C measurement error associated with the thermocouples after 5 h. However, after 10 h, the measurements and CFD results diverge with a maximum discrepancy of 1 °C between the reading from T7 and the associated CFD mesh node. Fig. 7 shows the evolving temperature profile for copper against the CFD results where the peak discrepancy rose to 1.1 °C after 10 h.

Once the model had been validated, the vector fields within the fluid domain of the simulation were examined. Fig. 8 shows the difference in simulated internal velocity fields for the copper and

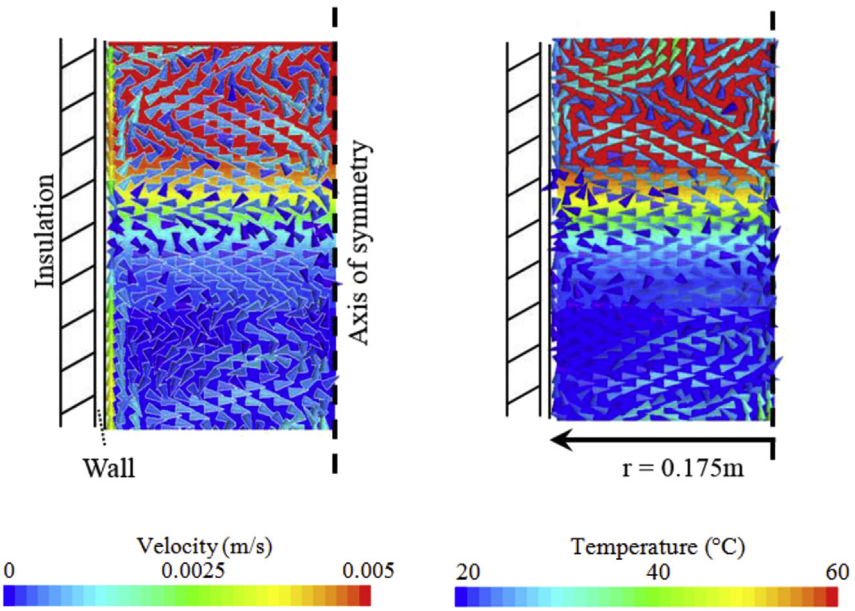

Fig. 8. Temperature and velocity fields around thermocline for copper (left) and stainless (right) walled 350 mm diameter tanks.

Please cite this article in press as: Armstrong P, et al., Improving the energy storage capability of hot water tanks through wall material specification, Energy (2014), http://dx.doi.org/10.1016/j.energy.2014.09.061

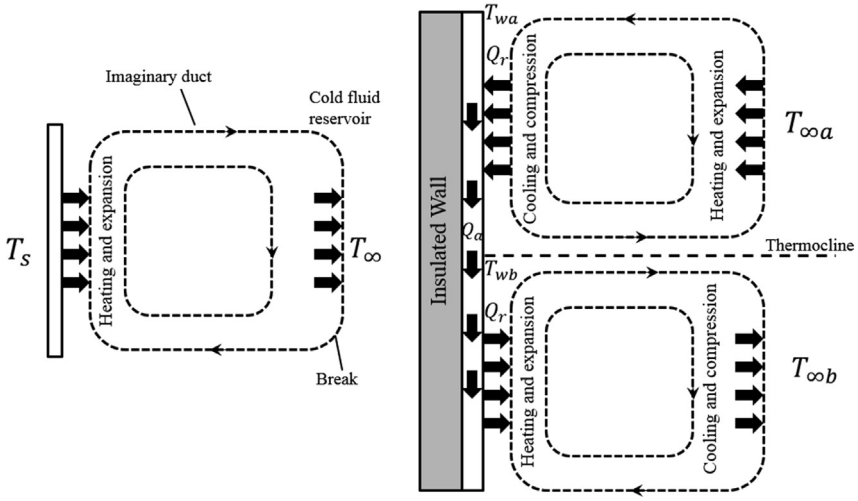

Fig. 9. (Left) heat engine analogy for natural convection presented in Ref. [83] (right) twin heat engine analogy applied to a conductive wall within a stratified fluid.

stainless tanks around the thermocline region. A convection system adjacent to the wall can be observed.

Two counter rotating currents can be seen above and below the thermocline, the pattern is more pronounced for the copper wall compared to the stainless. Peak velocities of 0.005 m/s and 0.003 m/s were observed in the copper and stainless tanks respectively; this is consistent with simulated velocities encountered in Ref. [31] which were found to be between 0.003 and 0.015 m/s. To explain the observation, we draw upon a heat engine analogy which is presented by Bejan [83] to describe the process of natural convection against a vertical heated wall (Fig. 9).

Bejan describes how fluid close to a heated surface, at temperature T_s, expands and rises before cooling and contracting within a cold reservoir adjacent to the wall at temperature T_∞. The CFD velocity field, indicated in Fig. 8, suggests an extension of this analogy whereby two separate heat engines, below and above the thermocline run clockwise and counter clockwise respectively as heat is transferred from the top of the tank to the bottom via a conductive wall, this is illustrated by the right hand side of Fig. 8. In this case, we have an adjacent cold reservoir at temperature $T_{\infty b}$ and an adjacent hot reservoir at $T_{\infty a}$.

The simulated radial heat flux exchange between the water and tank wall, Q_r, arising from the system illustrated by Fig. 9, is plotted on Fig. 10 against the temperature distribution, $T(x)$. Above the thermocline, the heat flux is negative reflecting the fact that heat is withdrawn from the fluid whilst beneath the thermocline, the heat flux is positive as the water below is heated. The peak value recorded for copper is 1858 W/m^2 compared to 356 W/m^2 for stainless and 25 W/m^2 for polyethylene. If we assume the heat losses from the tank wall to the environment to be negligible compared to the conjugate exchange with the water, then the net radial heat exchange should equal zero, we can therefore estimate the total axial heat transfer, Q_a, from the top of the tank to the bottom during de-stratification via the following equation:

$$Q_a \approx \int_0^H 1/2\,|Q_r(x)|dx \tag{21}$$

Q_a values of 181.5, 11 and 0.8 W for 1 mm walls made from copper, stainless and polyethylene were calculated respectively for a thermocline gradient of 400 K/m.

The thermocline gradient will depend on the geometry and thermal distribution associated with heat transfer surfaces within the tank, along with the passage of time during which the gradient drops. Table 4 presents the value of the measured thermocline gradient within the stainless and copper tanks after warm up alongside values found in the literature:

To determine the influence of the thermocline gradient, mesh wall node temperatures and water node temperatures from outside of the thermal boundary layer were taken alongside the wall radial heat flux values, $Q_r(x)$, to calculate the local heat transfer coefficient

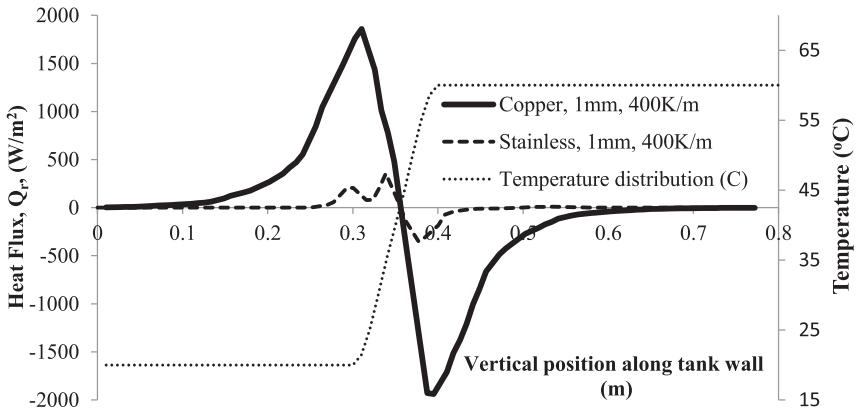

Fig. 10. Simulated radial heat flux exchange between wall and water for stainless and copper 1 mm walls with thermocline gradient of 400 K/m.

Please cite this article in press as: Armstrong P, et al., Improving the energy storage capability of hot water tanks through wall material specification, Energy (2014), http://dx.doi.org/10.1016/j.energy.2014.09.061

Table 4
Thermal gradients measured and sourced from the literature.

Experimental study	Maximum measured thermocline gradient (K/m)
Initial gradient in stainless tank	407
Initial gradient in copper tank	395
S. Alizadeh et al. [84]	297.5
J. Fernandezseara et al. [28]	174.7
E. M. Kleinbach et al. [62]	105.3
Jordan and Furbo [70]	286

$h(x)$. The values are shown in Fig. 11 for the 1 mm copper wall with thermocline gradients of 400 and 200 K/m.

The average local heat transfer coefficients were 205 W/m^2 and 202 W/m^2 for thermocline gradients of 400 K/m and 200 K/m respectively. Whilst $h(x)$ was relatively flat across most of the wall, there appeared to be a pronounced dip around the thermocline region, this is associated with reduced buoyancy driven flow which can be observed in Fig. 7. The magnitude of these values was checked against the values provided by the averaged Nusselt number, $\overline{N_u}$, for natural convection around a vertically heated plate given in Ref. [85]:

$$\overline{N_u} = 0.1R_a^{1/3} \text{ for } 10^9 < R_a < 10^{13} \tag{22}$$

where the Rayleigh number is given as:

$$R_a = \frac{g\beta(\overline{\Delta T})H^3}{\upsilon^2}P_r = G_rP_r \tag{23}$$

where: g is gravitational acceleration, β, is the volumetric expansion coefficient, $\overline{\Delta T}$ is the average temperature difference between the wall and water outside the thermal boundary layer measured from the CFD model, υ is the kinematic viscosity and G_r is the Grashoff number. The average heat transfer coefficient, $\overline{h}$, can then be given by:

$$\overline{h} = \frac{N_u k}{H} \tag{24}$$

Equation (18) yielded values of 180 and 166 W/m^{2}K for thermocline gradients of 400 and 200 K/m.

It has been shown that heat transfer correlations for cylindrical geometries are equivalent to results applied for flat plates providing the diameter to height ratio exceeds the following ratio [86]:

$$\frac{d}{H} \geq \frac{55}{G_r^{1/4}} \tag{25}$$

For the stainless tank tested and simulated in this paper, the RHS of (25) is $55/G_r^{1/4} = 0.28$ whereas $d/H = 0.44$ indicating that the heat transfer results discussed in this section would be applicable for both flat plates and cylinders where the above condition is met and where $10^9 < R_a < 10^{13}$.

With the CFD simulation validated by the stainless test tank, along with the check that values seemed reasonable against those produced by the correlations described in (22), the CFD model was run for the different material choices involving: copper, stainless and polyethylene. Results for both perfect wall insulation (adiabatic) and tanks insulated with 50 mm of polyurethane foam with T_a = 15 °C over a period of 12 h were produced. These results, alongside measurements from the test tanks, are presented in Fig. 12 and Table 5.

As had been observed during experiment, the CFD results indicated an approximately linearly relationship between decreasing useable volume and time over 12 h with R^2 values provided in Table 4. The CFD model was consistent with the stainless test tank to within ± 1.3 L and ± 1.2 L for the copper tank over the duration of the 12 h run.

Table 4 shows that the selection of stainless over copper for a 1 mm wall decreased useable volume loss by a factor of 2.7 with a switch from copper to polyethylene yielding a 5 fold reduction. Perfect insulation of a 1 mm stainless wall resulted in a 9.4% reduction in usable volume loss compared to 50 mm of Polyurethane with a reduction of 64% for copper.

Equations (1)–(3) were applied to estimate the pressure rating of the vertical wall section with a factor of safety of 3 using the ultimate tensile strength values specified in Table 1. 1 mm grade polyethylene could withstand less than 1 bar of pressure making it unsuitable without reinforcement whereas stainless could withstand more than 9 bar of pressure.

8. Discussions and conclusions

The experimental and numerical findings in this paper clearly demonstrate that the use of copper as a wall material results in a significant increase in the rate of de-stratification during the tank's static mode of operation. Total loss of useable hot water occurred after 28 h for the copper tank under test compared to 42 h for the stainless unit which had the same volume and overall diameter. The consequences of this are that during operation, the copper tank would be less capable as a store of intermittent energy on a renewable or flexible tariff scheme since the heating element

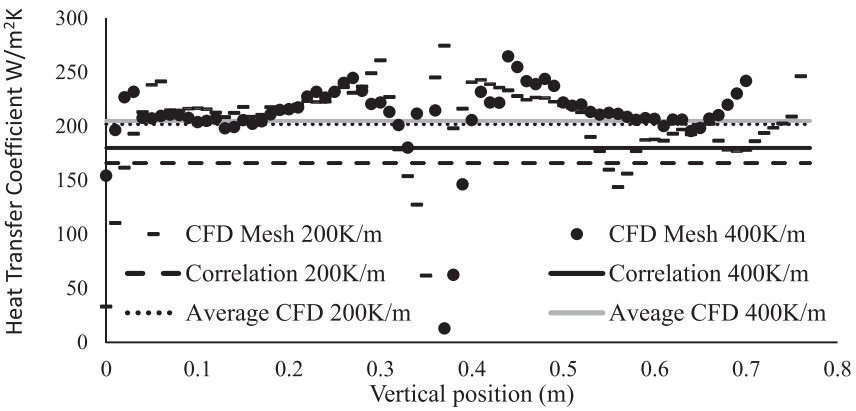

Fig. 11. Simulated local heat transfer coefficient for 1 mm copper wall alongside averaged analytical flat plate correlations based on mean wall water temperature difference.

Please cite this article in press as: Armstrong P, et al., Improving the energy storage capability of hot water tanks through wall material specification, Energy (2014), http://dx.doi.org/10.1016/j.energy.2014.09.061

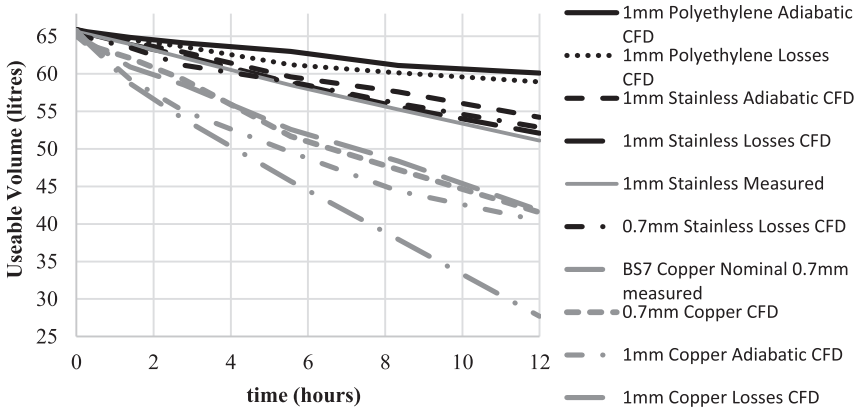

Fig. 12. Simulated and measured useable volume loss curves for stainless, copper and polyethylene materials.

would have to fire more frequently to maintain an adequate volume of hot water for the end user. Further work is required to quantify the system costs associated with de-stratification in hot water tanks within energy systems against different draw cycles along with the extent to which improved standing thermal performance can lead to better utilization of renewable energy sources.

A 2D axi-symmetric CFD model was validated against the measurements taken from the stainless and copper test tanks. This model runs much faster than a 3D equivalent allowing for an exploration of alternative wall materials. The numerical results showed that the selection of stainless over copper, for a 1 mm thick wall, decreased useable volume loss by a factor of 2.7 with a switch from copper to polyethylene yielding a 5 fold reduction. In addition to this, the lower cost of stainless compounded with its higher tensile strength means that for mains pressurized systems operating up to 6.5 bar, a lighter, thinner, stainless wall within a UK tank would be less than a sixth of the material cost in comparison to its copper equivalent; further analysis is required to account for the additional manufacturing costs associated with stainless due to its higher melting temperature and stiffness. Whilst a polyethylene wall exhibits very low rates of de-stratification, it would have to be reinforced by additional materials. Further work is required to understand whether alternative low conductivity materials and composites could offer significant improvements in useable volume and exergy retention, one option may be stainless coated with vitreous enamel glass, this would lower thermal conductivity and be immune to the corrosion problems that have been encountered in enameled mild steel tanks.

The results discussed in this paper apply where the initial thermocline position was half way up the tank, in practice the thermocline shape and position will depend on the location of all thermal inputs along with the operation of the system over time. Further work is required to understand how these factors influence system performance against realistic draw cycles.

The evidence for copper as a sanitizing agent is inconclusive, whilst it has been shown to inhibit *legionella* under laboratory conditions, field work in the literature has found a positive association between copper tanks and *legionella* along with prolific bacterial growth. On the basis of this, along with the findings in this paper, it would seem that the superior thermal performance, reduced material cost and high tensile strength associated with stainless steel; makes it a preferable alternative to copper. Whilst the use of polyethylene would result in a lower rate of de-stratification compared to stainless, polyethylene has been associated with higher rates of biofilm growth and would require additional materials to compensate for its low tensile strength.

Reducing the thickness of stainless steel walls from 1 mm to 0.7 mm decreases useable volume loss by 13%, however the associated pressure rating falls to 6.3 bar which is beneath the rating of expansion relief valves in pressurized UK domestic systems [48]. This highlights the trade-off between material thickness, de-stratification, pressure rating and material cost when specifying the wall thickness. It is also crucial to consider the stress concentrations that arise towards the top and bottom ends of a hot water cylinder where the wall thicknesses must be increased. Further work should be undertaken to explore these trade-offs along with fabrication techniques that could optimize the wall grade without incurring unreasonable costs.

The CFD analysis provided further insight into the flow patterns that arise within the tank. Counter rotating convection currents were observed above and below the thermocline. This convection system was more pronounced for a copper wall compared to stainless or polyethylene due to the higher rate of heat flux that travels radially and axially through the wall. Future work could

Table 5
Simulated and measured rates of useable volume and exergy loss within test tanks for different wall materials and thicknesses.

Material type/thickness	Useable volume loss rate over 12 h (liters/hour) (R^2)	Initial internal exergy (MJ)	Final internal exergy (MJ)	Exergy loss (%)	Maximum tank wall operating pressure (bar)
1 mm copper with losses (CFD)	3.12 (0.99)	1.06	0.412	39	4.4–6.6
BS7 tank 0.7 mm copper nominal (measured)	2.10 (0.95)	1.06	0.69	35	3–4.6
0.7 mm copper CFD	2.11 (0.99)	1.05	0.68	35	3–4.6
1 mm copper adiabatic (CFD)	1.91 (0.99)	1.08	0.77	29	4.4–6.6
1 mm stainless (Measured)	1.18 (0.98)	1.07	0.80	25	9.1
1 mm stainless with losses (CFD)	1.16 (0.99)	1.08	0.82	24	9.1
0.7 mm stainless with losses (CFD)	1.03 (0.99)	1.06	0.85	21	6.3
1 mm stainless adiabatic (CFD)	0.97 (0.99)	1.08	0.97	10.2	9.1
1 mm polyethylene with losses (CFD)	0.60 (0.96)	1.08	0.84	22	0.3–0.8
1 mm polyethylene adiabatic (CFD)	0.49 (0.99)	1.08	0.99	8.3	0.3–0.8

Please cite this article in press as: Armstrong P, et al., Improving the energy storage capability of hot water tanks through wall material specification, Energy (2014), http://dx.doi.org/10.1016/j.energy.2014.09.061

examine whether this physical insight can lead to the formulation of more accurate heat transfer correlations for conductive walls immersed in stratified fluids, this would improve the accuracy of one dimensional stratification models allowing the implications of standing thermal performance of hot water tanks to be understood over larger time-scales within the context of a power system.

Acknowledgments

The authors wish to acknowledge the support from CD Adapco who assisted with the CFD models along with Mark Smith at Newark Copper cylinder for his help in the design and build of the test tanks. We are also indebted to Robin Vincent at Oxford University who helped in the fabrication of the water temperature probes. Finally we are indebted to the UK's Engineering and Physical Sciences Research Council (D4TD4D11) who funded this research.

References

[1] Palmer J, Cooper I. Great Britain's housing energy fact file. Dep. Energy Clim. Chang.; 2011. p. 28.
[2] van Blommestein KC, Daim TU. Residential energy efficient device adoption in South Africa. Sustain Energy Technol Assess Mar. 2013;1:13–27.
[3] Bagge H, Johansson D. Measurements of household electricity and domestic hot water use in dwellings and the effect of different monitoring time resolution. Energy May 2011;36(5):2943–51.
[4] Pina A, Silva C, Ferrão P. The impact of demand side management strategies in the penetration of renewable electricity. Energy May 2012;41(1):128–37.
[5] Atikol U. A simple peak shifting DSM (demand-side management) strategy for residential water heaters. Energy Dec. 2013;62:435–40.
[6] Electricity supply in the United Kingdom, a chronology. 4th ed. Chatham: The Electricity Council; 1987. p. 127.
[7] Stephan A, Stephan L. Reducing the total life cycle energy demand of recent residential buildings in Lebanon. Energy Aug. 2014;74:618–37.
[8] Fehrenbach D, Merkel E, McKenna R, Karl U, Fichtner W. On the economic potential for electric load management in the German residential heating sector – an optimising energy system model approach. Energy May 2014;71:263–76.
[9] Buonomano A, Calise F, Ferruzzi G. Thermoeconomic analysis of storage systems for solar heating and cooling systems: a comparison between variable-volume and fixed-volume tanks. Energy Sep. 2013;59:600–16.
[10] Dincer I, Rosen MA. Thermal energy storage systems and applications. 2nd ed. Wiley; 2002. p. 238.
[11] Lindley D. Smart grids: the energy storage problem. Nature January, 2010;463.
[12] Okou R, Sebitosi a B, Pillay P. Flywheel rotor manufacture for rural energy storage in sub-Saharan Africa. Energy Oct. 2011;36(10):6138–45.
[13] Poullikkas A. A comparative overview of large-scale battery systems for electricity storage. Renew Sustain Energy Rev Nov. 2013;27:778–88.
[14] Kim C, Member S, Kim M, Member S. A modularized charge equalizer using a battery monitoring IC for series-connected Li-ion battery strings in electric vehicles 2013;28(8):3779–87.
[15] Thibaut K. Elon Musk: supercapacitors not batteries, will be breakthrough for EVs. Tech Crunch; 2011 [Online]. Available from: http://techcrunch.com/2011/03/25/elon-musk-says-super-capacitors-not-batteries-will-be-breakthrough-for-evs/ [accessed 15.09.14].
[16] David LaGesse. Supercapacitors Amp Up as an alternative to batteries. National Geographic; 2013 [Online]. Available from: http://news.nationalgeographic.com/news/energy/2013/08/130821-supercapacitors/.
[17] Chuckwuka C, Folly KA. Batteries and super-capacitors. In: IEEE PES; 2012. p. 9–13. no. July.
[18] Albright G, Edie J, Al-Hallaj S. A comparison of lead acid to lithium-ion in stationary storage applications contributors. 2012. no. March.
[19] Measurement of domestic hot water consumption in dwellings. 21 Dartmouth Street, London: Energy Saving Trust; 2008. SW1H 9BP, http://www.energysavingtrust.org.uk.
[20] Armstrong PM, Ager D, Thompson I, McCulloch MD. Domestic hot water storage: balancing thermal and sanitary performance (accepted 2014). Energy Policy 2014.
[21] Turner J. Buoyancy effects in fluids. 1st ed. Cambridge: Cambridge University Press; 1979. p. 4.
[22] Cole RL, Bellinger FO. Natural thermal stratification in tanks. Final Report. Argonne Natl. Lab.; 1982.
[23] Fan J, Furbo S. Thermal stratification in a hot water tank established by heat loss from the tank. Sol Energy Nov. 2012;86(11):3460–9.
[24] Castell A, Medrano M, Solé C, Cabeza LF. Dimensionless numbers used to characterize stratification in water tanks for discharging at low flow rates. Renew Energy Oct. 2010;35(10):2192–9.
[25] Fernández-Seara J, Uhı́a FJ, Sieres J. Experimental analysis of a domestic electric hot water storage tank. Part II: dynamic mode of operation. Appl Therm Eng Jan. 2007;27(1):137–44.
[26] Chauvet L, Probert S, Nevrala D. Thermal-energy stores for supplying domestic hot-water and space-heating. Appl Energy 1994;48(ii):163–90.
[27] Hariharan K, Badrinarayana K, Srinivasa Murthy S, Krishna Merthy M. Temperature stratification in hot-water storage tanks. Energy 1991;16(7):977–82.
[28] Fernandezseara J, Uhia F, Sieres J. Experimental analysis of a domestic electric hot water storage tank. Part I: static mode of operation. Appl Therm Eng Jan. 2007;27(1):129–36.
[29] Abdolyt MA, Rapp D. Theoretical and experimental studies of stratified thermocline storage of hot water. Energy Convers Manage 1982;22(Iii):275–85.
[30] Klein SA, Beckman WA. TRNSYS 16: a transient system simulation program: mathematical reference. TRNSYS 2007;5:389–96.
[31] Fan J, Furbo S. Buoyancy driven flow in a hot water tank due to standby heat loss. Sol Energy Nov. 2012;86(11):3438–49.
[32] British Standard 699:1984. Copper direct cylinders for domestic purposes. The British Standards Institute; 1990.
[33] Taylor P, Waines PL, Moate R, Moody AJ, Allen M, Bradley G. Biofouling: the journal of bioadhesion and biofilm. The effect of material choice on biofilm formation in a model warm water distribution system. Biofouling no. March. 2012. p. 37–41.
[34] Mathys W, Stanke J, Harmuth M, Junge-Mathys E. Occurrence of Legionella in hot water systems of single-family residences in suburbs of two German cities with special reference to solar and district heating. Int J Hyg Environ Health Mar. 2008;211(1–2):179–85.
[35] V Lee J, Bartram J, Chartier Y, Pond K, Surmann-Lee S. Legionella and the prevention of legionellosis. World Heal. Organ.; 2008.
[36] Armstrong PM, Uapipatanakul M, Thompson I, Ager D, McCulloch M. Thermal and sanitary performance of domestic hot water cylinders: conflicting requirements. Appl Energy Oct. 2014;131:171–9.
[37] London metal exchange online – copper price time series. [Online]. Available from: http://www.lme.com/, [accessed January 2014].
[38] Metal prices online: stainless steel price time series. [Online]. Available from: www.metalprices.com, [accessed January 2014].
[39] Platts McGraw Hill Financial: global petrochemical index. [Online]. Available from: http://www.platts.com/news-feature/2013/petrochemicals/pgpi/ldpe, [accessed January 2014].
[40] Colbourne JS, Avenue R, Ecr L. Water fittings as sources of Legionella Pneumophila in a hospital plumbing system. Lancet 1984;323(8370):210–3.
[41] Schofield GM, Locci R. Colonization of components of a model hot water system by Legionella pneumophila. J Appl Bacteriol Feb. 1985;58(2):151–62.
[42] Brundett G. Legionnaires' disease building services – healthy buildings. Build Res Pract J CIB 1989;(2):96–107.
[43] Brenner S. Aluminium, hot water tanks and neurobiology. Lancet 1989;1(8641):781.
[44] Rondeau V, Commenges D, Jacqmin-gadda H, Dartigues J. Relation between aluminum concentrations in drinking water and Alzheimer's disease: an 8-year follow-up study 2000;152(1):59–66.
[45] van der Kooij D, Veenendaal HR, Scheffer WJH. Biofilm formation and multiplication of Legionella in a model warm water system with pipes of copper, stainless steel and cross-linked polyethylene. Water Res Aug. 2005;39(13):2789–98.
[46] Conversations with UK hot water tank manufacturers.
[47] Vasiliev VV, Krikanov a a, Razin a F. New generation of filament-wound composite pressure vessels for commercial applications. Compos Struct Jan. 2003;62(3–4):449–59.
[48] British Standard BS 7206:1990. Unvented hot water storage units and packages. The British Standards Institute; 1990.
[49] Williams M, Todd J. Structures, theory and analysis. Wiltshire: Macmillan Press Ltd.; 2000. p. 125.
[50] Williams M, Todd J. Structures, theory and analysis. Wiltshire: Macmillan Press Ltd; 2000. p. 286–314.
[51] Mat-Web, materials database – polyethylene entry. [Online]. Available from: http://www.matweb.com/search/DataSheet.aspx?MatGUID=f9470672aa5549cb9c7b157677d02062. [accessed 16.02.14].
[52] Nwosu PN, Agbiogwu D. Thermal analysis of a novel fibre-reinforced plastic solar hot water storage tank. Energy Oct. 2013;60:109–15.
[53] Endless-Solar. Technical Note: Vitreous Enamel versus Stainless Steel Tanks. Sydney. 2014.
[54] Newton BJ. Modelling of solar storage tanks. Master's Thesis. University of Wisconsin-Madison; 1995.
[55] Mat-Web, materials database – copper entry. [Online]. Available from: http://www.matweb.com/search/DataSheet.aspx?MatGUID=9aebe83845c04c1db5126fada6f76f7e. [accessed 16.02.14].
[56] British Standard EN 1172:1996. Copper and copper alloys – sheet and strip for building purposes. The British Standards Institute; 1997.
[57] Mat-Web, materials database – stainless steel entry. [Online]. Available from: http://www.matweb.com/search/DataSheet.aspx?MatGUID=ace15139b9e846a493dc630db9dac567&ckck=1. [accessed 16.02.14].
[58] British Standard BS 7291-3:2006. Thermoplastic pipes and associated fittings for hot and cold water for domestic purposes and heating installations in buildings. The British Standards Institute; 2006.
[59] British Standard BS EN 14318-1:2013. In-situ formed dispensed rigid polyurethane and polisocyanurate foam products. British Standards Institute; 2013.

Please cite this article in press as: Armstrong P, et al., Improving the energy storage capability of hot water tanks through wall material specification, Energy (2014), http://dx.doi.org/10.1016/j.energy.2014.09.061

[60] Cengel YA, Boles MA. Thermodynamics: an engineering approach. 5th ed. McGraw Hill; 2006. p. 309.
[61] Zurigat YH, Maloney K, Ghajar A. A comparison study of one-dimensional models for stratified thermal storage tanks. Trans ASME 1989;111:204–10.
[62] Kleinbach EM, Beckman WA, Klein SA. Performance study of one-dimensional models for stratified thermal storage tanks. Sol Energy Feb. 1993;50(2):155–66.
[63] Kaloudis E, Grigoriadis DGE, Papanicolaou E, Panidis T. Large eddy simulations of turbulent mixed convection in the charging of a rectangular thermal storage tank. Int J Heat Fluid Flow Dec. 2013;44:776–91.
[64] Khalifa AJN, Mustafa AT, Khammas FA. Experimental study of temperature stratification in a thermal storage tank in the static mode for different aspect ratios. ARPN J Eng Appl Sci 2011;6(2):53–60.
[65] Angel C. Guidance controlling scalding risks from bathing and showering. United Kingdom Home Care Assoc.; 2012. p. 1–12. no. 3083104.
[66] Bejan A. Convection heat transfer. 4th ed. New Jersey: Wiley; 2013. p. 210–1.
[67] Edwards DK, Catton I. Prediction of heat transfer by natural convection in closed cylinders heated from below. J Heat Mass Transf 1968;12:22–30.
[68] Lameiro GF, Duff WS. A Markov model of solar energy space and hot water heating systems. Sol Energy 1979;22.
[69] Lacroix M. Electric water heater designs for load shifting and control of bacterial contamination. Energy Convers Manage Aug. 1999;40(12):1313–40.
[70] Jordan U, Furbo S. Thermal stratification in small solar domestic storage tanks caused by draw-offs. Sol Energy Feb. 2005;78(2):291–300.
[71] Sterling SJ, Collins MR. Feasibility analysis of an indirect heat pump assisted solar domestic hot water system. Appl Energy May 2012;93:11–7.
[72] Fan J, Furbo S. Thermal stratification within a hot water tank established by heat loss of the tank. In: Proc. ISS Sol. World Congr. 2009 Renew. Energy Shap. Our Futur.; 2009. p. 341–50.
[73] Versteeg WMHK. An introduction to computational fluid dynamics the finite volume method. 2nd ed. p. 9.
[74] Star CCM+ multiphysics software. CD Adapco; 2014 [Online]. Available from: http://www.cd-adapco.com/products/star-ccm® [accessed 23.02.14].
[75] Chung T. Computational fluid dynamics. 1st ed. Cambridge: Cambridge University Press; 2002. p. 305–6.
[76] Oliveski RDC, Macagnan MH, Copetti JB, Petroll ADLM. Natural convection in a tank of oil: experimental validation of a numerical code with prescribed boundary condition. Exp Therm Fluid Sci Jul. 2005;29(6):671–80.
[77] Pieter W. Principles of computational fluid dynamics. 1st ed. Berlin: Springer; 1991. p. 46.
[78] Gray DD, Giorcini A. The validity of the Boussinesq approximation for liquids and gases. Heat Mass Transf 1976;19:545–51.
[79] Armstrong P, McCulloch M. Distributed energy storage using domestic hot water tanks and a novel thermocline sensor (accepted). In: IEEE ISGT; 2014.
[80] Least-squares (model fitting) algorithms. Matlab Documentation Centre; [Online]. Available from: http://www.mathworks.co.uk/help/optim/ug/least-squares-model-fitting-algorithms.html.
[81] Andrew N. Stanford machine learning course: linear regression with multiple variables (week 2). Coursera; 2013 [Online]. Available from: https://class.coursera.org/ml-003/lecture/preview.
[82] Taylor JR. An introduction to error analysis. 2nd ed. Colorado: University Science Books; 1997. p. 45–79.
[83] Bejan A. Convection heat transfer. 4th ed. 2013. p. 168–9. New Jersey.
[84] Alizadeh S. An experimental and numerical study of thermal stratification in a horizontal cylindrical solar storage tank. Sol Energy Sep. 1999;66(6):409–21.
[85] Bahrami M. Natural convection, heat transfer course notes. Simon Fraser University; 2014 [Online]. Available from: http://www.sfu.ca/~mbahrami/ENSC 388/Notes/Natural Convection.pdf [accessed: 23.02.14].
[86] Fernández-Seara J, Uhía FJ, Alberto Dopazo J. Experimental transient natural convection heat transfer from a vertical cylindrical tank. Appl Therm Eng Aug. 2011;31(11–12):1915–22.

Please cite this article in press as: Armstrong P, et al., Improving the energy storage capability of hot water tanks through wall material specification, Energy (2014), http://dx.doi.org/10.1016/j.energy.2014.09.061